

# Unsupervised Discrimination of Motor Unit Action Potentials Using Spectrograms

Thuy T. Pham<sup>1,2</sup>, Andrew J. Fuglevand<sup>1</sup>, Alistair L. McEwan<sup>2</sup>, and Philip H.W. Leong<sup>2</sup>

**Abstract**—Single motor unit activity study is a major research interest because changes of MUAP morphology, MU activation, and MU recruitment provide the most informative part in diagnosis and treatment of neuromuscular disorders. Intramuscular recordings often provide a more than one motor unit activities, thus MUAP discrimination is a crucial task to study single unit activities. Most neurology laboratories worldwide still need specialists who spend hours to classify MUAPs. In this study, we present a new real-time unsupervised method for MUAP discrimination. After automatically detect MUAPs, we extract features of spectrogram images from the wavelet coefficients of MUAPs. Unlike benchmark methods, we do not calculate Euclidean distances which assumes a spherical distribution of data. Instead, we measure correlation between spectrogram images. Then MUAPs are automatically discriminated without any prior knowledge of the number of clusters as in previous works. MUAP were detected on a real data set with a precision *PPV* of 94% (tolerance of 2 ms). We obtained a similar result in MUAP classification to the reference. The difference in percentages of MU proportions between our method and the reference were 3% for MU1, 0.4% for MU2, and 12% for MU3. In contrast, F1-score for MU3 reached the highest level at 91% (*PPV* at the highest of 96.64% as well).

## I. INTRODUCTION

Motor unit activity analysis provides the most informative part in diagnosis and treatment of neuromuscular disorders. In intramuscular electromyography data, a motor unit action potential (MUAP) consists of several muscle fiber action potentials within the anatomical motor unit (MU). A single MU activity is of research interest because changes of MUAP morphology, MU activation, and MU recruitment yield valuable information. Neuropathic conditions happen with decreased recruitment whereas myopathic conditions happen with MUAP morphology changes. Therefore, as an example, a MUAP examination can confirm myopathic conditions and identify the differential to find an appropriate biopsy site [1]. On the other hand, most neurology laboratories worldwide still need experts who spend hours on classifying action potentials (“spikes”) using commercial software tools (e.g. Spike2 [2], Cerebus [3]) after each recording. Hence, a real-time unsupervised method is highly desirable.

A practical spike discrimination procedure involves three basic phases: spike detection, feature extraction, and spike clustering. Spike detection processes have been performed by three typical groups: threshold-based method, energy-based

method, or template-based method. Though the threshold-based one performs simple computation, it is sensitive to noise [4]. The energy-based group which often uses a non-linear energy operator (NEO)[5] to estimate the square of the instantaneous product of amplitude and frequency of signal is the most supported method [4] and is selected in this study. Feature extraction algorithms have been reviewed recently in [6] and [7]. Primitive techniques that used only very simple features are subject to noise and/or inherent variation in spike morphology. Among recent sophisticated methods, principal component analysis (PCA) [8] still is the most popular with very high accuracy though it is not for a real-time process and has a high computational cost. Whereas, the discrete wavelet transform (DWT) [9] that localizes well in both time and frequency achieves fairly high accuracy at a relatively high cost [7]. According to an early review of clustering algorithms by Lewicki [10] and a recent one by Gibson et al. [7], the current benchmark method is K-means clustering [11] because it is simple and fast but not unsupervised. The valley-seeking [12] and super paramagnetic clustering (SPC) [13] are unsupervised and nonparametric but are not real-time and have high complexity [7]. For example, SPC also requires default settings of running 100 Monte Carlo iterations that increases computation time. Most of these techniques use the Euclidean distance metric that must assume a spherical distribution of data. In fact, due to the effect of electrode drift, ellipsoidal clusters are formed, not spherical [7].

In this work, we propose a new real-time automatic non-parametric method. We extracted a new feature set of spikes to improve the performance. Instead of using Euclidean distances as in previous works, we calculate the correlation between spectrogram images learned from a short Fourier transform (STFT [14]). Then MUAPs are automatically discriminated without any prior knowledge of the number of clusters.

## II. ALGORITHMS

### A. MUAP Detection

Intramuscular data is corrupted by spike-like correlated noise. Thus, we need to make data points statistically independent (“pre-whitening”). A practical approach is using a linear prediction filter [15] and whiten the input signal itself before we extract any MUAP. In this work, we use a third-order forward linear predictor (FIR filter) that predicts the current value of the real-valued original data based on past three samples.

<sup>1</sup>T. Pham, A. McEwan, and P. Leong are with the Department of Electrical and Information Engineering, University of Sydney, NSW, Australia.

<sup>2</sup>T. Pham and A. Fuglevand are with the Department of Physiology, University of Arizona, AZ, USA.

We employ NEO to find changes in the energy of the recording signal. NEO can provide the instantaneous energy of the high pass filtered version of a signal. This feature makes NEO an ideal detector of transients [16]. Let  $x(t)$  be a real process which is band limited with a spectrum  $S_{xx}(w) = 0$  for  $|w| > B$  and  $x(nT)$  be the uniformly sampled version of  $x(t)$  with a sampling interval  $T < \frac{\pi}{B}$ . For convenience,  $T$  is dropped from the discrete time notations. For the discrete time version  $x(n)$ , the non-linear energy operator  $\psi[x(n)]$  is defined by Kaiser [5] with an general adjacent time  $\delta$  as  $\psi[x(n)] = x^2(n) - x(n+\delta)x(n-\delta)$ . From the interpretation by Mukhopadhyay et al. [16], the expectation value of  $\psi[x(n)]$  will be much greater than a threshold level whenever a spike appears because a spike is characterized by localized high frequencies and an increase in instantaneous energy. Most NEO-based spike detection algorithms introduce a threshold level  $\Theta$  (1). The NEO operation increases the signal to noise ratio therefore the detection result is less sensitive to  $\Theta$  than methods that look only at changes in amplitude or energy without regarding the frequency. This detection method is unsupervised as the threshold can be set automatically and also in real time with a small delay for buffering or the initial calculation period.

$$\Theta = C \frac{1}{N} \sum_{n=1}^N \psi[x(n)] \quad (1)$$

where  $C$  is a constant which is used to tune  $\Theta$ , and  $N$  is the number of samples.

### B. Feature Extraction

According to reviews [6][7], we extract MUAP features with a reduced dimension by using both the DWT technique [9] and a K-S test [17]. Basically, to find differences among spikes, DWT is based on the quantification of energy found in specific frequency bands at specific time locations. Let  $s(t)$  be a spike waveform which can be presented by coefficients  $C(a, b) = \frac{1}{\sqrt{a}} \int_{-\infty}^{+\infty} s(t) \psi_{a,b}(t) dt$  where  $\psi_{a,b}(t) = \psi\left(\frac{t-b}{a}\right)$  is an expanded or contracted and shifted version of a unique wavelet function  $\psi(t)$   $a$  and  $b$  are the scale and the time localization, respectively. In the next steps, we apply a dynamic spectral analysis that does not assume a stationary signal as in conventional spectral analysis method but only a segment of signal. It creates a series of spectral snapshots (spectrogram) for every spike's compressed coefficient set. STFT is the mathematical technique to produce spectrograms. Let  $x[n]$  be an input vector to be transformed.  $x[n]$  is broken up into frames (size  $m$ ). Frames should overlap each other to avoid artifacts at the boundary. This transform can be expressed as in (2) and spectrogram  $\{x(n)\}(m, \omega) \equiv |X(m, \omega)|^2$ .

$$X(m, \omega) = \sum_{n=-\infty}^{\infty} x[n] h[n-m] e^{-j\omega n} \quad (2)$$

where  $x[n]$  is an input of the transform,  $h[n]$  is a window function with size  $m$ .

### C. MUAP Clustering

To evaluate with a contemporary method later in Section III, we first describe a brief algorithm for SPC. The SPC method is compared here as it also uses wavelet coefficients to classify but not a further spectrogram analyzing step. SPC represents  $m$  features of a spike  $i$  by a point  $x_i$  in an  $m$ -dimensional space. Then it finds the interaction strengths  $J_{ij}$  between the point  $x_i$  and one of  $k$  nearest neighboring points (3 [18]).  $J_{ij}$  reduces exponentially when the Euclidean distance  $\|x_i - x_j\|^2$  increases. A smaller distance results in a stronger similarity between two spikes. After that, SPC assigns each point  $x_i$  to a random state  $s$  in a set of  $q$  states. Then,  $N$  Monte Carlo iterations are run for different temperatures using the Swendsen-Wang algorithm [19].

$$J_{ij} = \begin{cases} \frac{1}{K} \exp\left(-\frac{\|x_i - x_j\|^2}{2a^2}\right) & \text{if } x_i \text{ is a neighbor of } x_j \\ 0 & \text{otherwise.} \end{cases} \quad (3)$$

where  $a$  is the average distance from  $x_i$  to its  $K$  nearest neighbors.

After extracting features of MUAPs by multi-resolution analysis in both time and frequency, instead of using the Euclidean distance metric, to account for electrode drift in our own method, we measure the correlation between spectrogram images. Let  $X$  and  $Y$  be two feature vectors of MUAP  $X$  and MUAP  $Y$ , respectively. The correlation degree  $r_{X,Y}$  between  $X$  and  $Y$  is calculated as  $r_{X,Y} = \frac{\mathcal{C}\{X,Y\}}{\sigma_X \sigma_Y}$  where  $\mathcal{C}\{X,Y\}$  is the covariance of  $X$  and  $Y$ .  $\sigma_X$  and  $\sigma_Y$  are the variances of  $X$  and  $Y$ , respectively. Then  $r_{X,Y}$  is one of the inputs to classify automatically MUAPs into appropriate clusters (Algorithm 1).

---

#### Algorithm 1 Correlation-based Clustering

---

```

function [C, Outliers]= clustering(S, F, Θco)
  i = 0; num = 0; y = [1]; sorted=nil; % initial
  bin=S(2:end,:); % matrix of N spikes
  While (size(bin,1) ≠ 0)
    i = i + 1;
    z = find(y == i, 1); % take unsorted spikes
    If (z is not empty) then
      num = num + 1; C{num}=nil; % create new class
      x = find(F(i,:)) ≥ Θco; % take high correlated
      x is added to sorted;
      F(i,sorted) = 0; % clear sorted spikes
      If (isempty(x)) then S{x,:} is added to C{num};
      Else Outliers=bin; EndIf; % last remaining
      bin=S(y,:); % temp remaining
    End of If; End of while;
  End;

```

---

The whole process of MUAP sorting (Algorithm 2) can be implemented online with a small delay of the first buffering duration. Let  $X$  be a buffered data segment (1 minute long) from a recording channel. The spike set  $S$  and its feature  $F$  are learned from NEO-based MUAP detection method (Section II-A) and spectrogram-based feature extraction procedure (Section II-B).  $M$  clusters of successfully sorted MUAPs are determined completely in an unsupervised

---

**Algorithm 2** MUAP sorting
 

---

```

function [C, Outliers]= sorting(data, fs, w,  $\Theta_{co}$ )
  i=1;
  While (i ≤ length(X))
    i = i + w; X = data(i : i + w); % buffering
    X = Prewhitening(X); % denoise
    S = NEO-based MUAP detection(X); % set of N spikes
    Spec = Spectrogram-of-DWT(S); % N images
    F = Correlation calculation(Spec); %  $r_{X,Y}$  of N images
    [C, Outlier] = Correlation-based Clustering(S, F);
    Online display(C, Outlier); % if requested
  End;
End;

```

---

TABLE I  
PERFORMANCE OF MUAP DETECTION.

Tolerance	TP	TN	FP	FN
0.5	939	7379623	609	519
2	1437	7123838	97	21
2.5	1451	7042723	84	7
5	1458	6688282	50	0

manner through the whole experiment without any priori knowledge of the number of clusters as in previous works.

### III. EXPERIMENTS

#### A. Data Set

We collected a real data set recording from a healthy young male at the Fuglevand Laboratory [20]. We used a rack-mounted electrophysiological recording system CED [2]. The electrode type was the concentric needle electrode. A neurologist expert worked on this data set and provide labels of when a MUAP appear and which MU it belongs to. The specialist used a commercial software tool (Spike2 [2]) and manually executed a template matching method. We used this labeling result as a “references” to evaluate our work.

#### B. Results

MUAPs were detected with a precision (positive predictive value *PPV*) of 94% (2 ms tolerance). MUAPs which were recognized the same as in the labels were denoted as True Positives (TP). When a MUAP was recognized by our method but not by the specialist, we denoted it as a False Positives (FP). Instances that we failed to label as MUAPs but were annotated as such, were defined as False Negatives (FN). When our method and the annotation agreed that there was no MUAP present, the instance was counted as a True Negative (TN). Table I illustrates more detailed of these *TP*, *TN*, *FP*, and *FN* across a wide range of tolerance. The performance started being acceptable at a tolerance as little as 1 ms and was very high at 2 ms.

Fig. 1 presents a similar result in MUAP classification. There are three MUAP classes found in both methods. In term of MUAP morphology in each class, the mean MUAP waveforms for MUs were almost identical to the reference’s ones (Fig. 2). We named our clusters according to the names in the reference (e.g. MU1, MU2, MU3 in

TABLE II  
COMPARISON OF MU HISTOGRAMS.

	Reference proportions	Our proportions	F1-score*	PPV*
MU1	29.97%	26.91%	86.47%	91.39%
MU2	32.90%	32.43%	81.53%	96.07%
MU3	36.44%	24.25%	91.00%	96.64%

Note: \* Our method vs. the reference.

Fig. 2). The histograms of our MU records are also similar to the ones of the reference (Table II). The difference in percentages of MU proportions between our sorting method and the reference were 3% for MU1, 0.4% for MU2, and 12% for MU3. The higher disparity of MU3 histogram may partially come from a slightly larger number of MUAPs we detected. In term of the accuracy of timing for every MU contribution, we used both F1-score [21] and *PPV*. Sorting evaluation sustains an unbalance classification, F1-score and *PPV* are better measurements than conventional sensitivity and specificity. *PPV* of each MU indicates the probability that clustered MUAPs truly belong to that MU. Whereas, F1-score (calculated as  $\frac{2TP}{2TP+FP+FN}$ ) is the harmonic mean of precision and sensitivity. Table II depicts these evaluation results for every MU. In contrast with the aforementioned variation in MU proportions, F1-score for MU3 reached the highest level at 91% (*PPV* at the highest of 96.64% as well). In general, all performance measurements we achieved in this study are among of the most accurate outcome in spike sorting evaluation works.

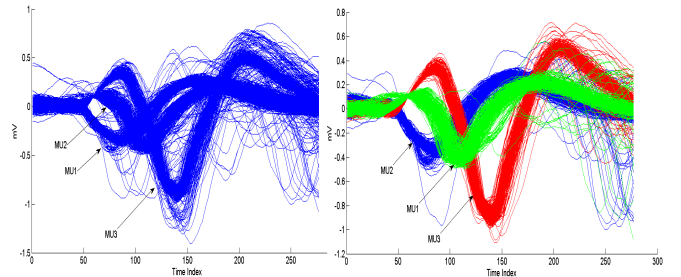


Fig. 1. Resemblance in MUAP classification by our method (left) and the reference (right).

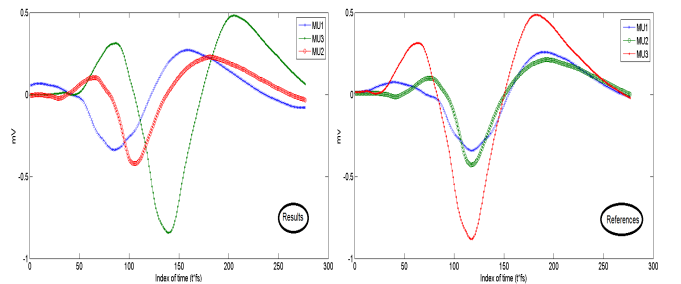


Fig. 2. Comparison of the mean MUAP waveforms for every MU between our method (left) and the reference (right).

Furthermore, we evaluated with SPC since it is a popular and high performance spike sorting method and it also uses

TABLE III  
MUAP SORTING EVALUATION.

	Our method	The SPC-based	The reference
Number of clusters (active MUs)	3	3 large + 3 small *	3
Total MUAPs	1534	1534	1468
MU1 MUAPs	395	422	440
MU2 MUAPs	356	394	483
MU3 MUAPs	476	414	535
Remaining MUAPs	307	304**	0

Note: \* The sizes are 66 (Class 4), 25 (Class 5), and 19 (Class 6)  
\*\* three small clusters + the remaining class (size of 194)

TABLE IV

MUAP SORTING ASSESSMENT OF OUR METHOD VS. THE SPC-BASED.

	Our method			The SPC-based		
	TP	FP	FN	TP	FP	FN
MU1	361	34	79	371	51	69
MU2	342	14	141	372	22	111
MU3	460	16	75	414	0	121

DWT coefficients as feature sets [7]. For the reason that SPC was designed for an offline method [7], we tested our method and the SPC-based method on one buffered data segment (2 minutes). Before running SPC, we had to pre-define an estimated number of valid clusters (e.g. 6 in our case). While our method automatically produces three similar clusters that are interpreted as active MUs to the ones of references, the SPC sorting need a further validation step by an operator. The operator need to discard the three invalid small clusters (Class4, Class5, and Class6) out of the six initially anticipated classes. Only after this step, the classification by all three methods agreed in the number of active MUs and their histograms (Table III). Though the MU proportions formed by the SPC seems a closer to the reference proportions, Table IV revealed a disparity of TP, FP, and FN. Our method achieved much more TPs and much less FNs than the SPC did for MU3. As for MU1 and MU2, the SPC got a slightly better TPs and FNs but much more in false positives.

#### IV. CONCLUSION

In summary, this paper proposes a real-time unsupervised and nonparametric method to discriminate motor unit action potentials. We tested our method on a real data set that recorded by a team of our group. MUAPs were detected with a precision *PPV* of 94% (2 ms tolerance). We obtained a similar result in MUAP classification to the reference. Three MUs were found in both methods. MUAP morphology is identical in each pair of corresponding MUs. The histograms of our MU records are also similar to the ones of the reference. The difference in percentages of MU proportions between our sorting method and the reference were 3% for MU1, 0.4% for MU2, and 12% for MU3. The higher disparity of MU3 histogram may partially come from a slightly larger number of MUAPs we detected. We used both F1-score [21] and *PPV* to measure the accuracy of timing for every MU contribution. In contrast with the aforementioned

variation in MU proportions, F1-score for MU3 reached the highest level at 91% (*PPV* at the highest of 96.64% as well).

While our method automatically produce three similar clusters that are interpreted as active MUs to the ones of references, the SPC sorting needs a further validation step by an operator. We found that this step may limit application of SPC in motor unit analyzing as we need to re-define this number when the number of active MUs is larger than we anticipated at the beginning. Our method does not encounter this problem and also reaches a high performance.

#### REFERENCES

- [1] S. Paganoni and A. Amato, "Electrodiagnostic evaluation of myopathies," *Physical medicine and rehabilitation clinics of North America*, vol. 24, no. 1, pp. 193–207, 2013.
- [2] *Cambridge Electronic Design: Spike2*, <http://www.ced.co.uk/>.
- [3] *Cerebus*, [www.cyberkineticsinc.com/](http://www.cyberkineticsinc.com/).
- [4] I. Obeid and P. Wolf, "Evaluation of spike-detection algorithms for a brain-machine interface application," *Biomedical Engineering, IEEE Transactions on*, pp. 905–911, 2004.
- [5] J. Kaiser, "On a simple algorithm to calculate the 'energy' of a signal," in *Acoustics, Speech, and Signal Processing, 1990. ICASSP-90., 1990 International Conference on*, vol. 1, 1990, pp. 381–384.
- [6] S. Gibson, J. W. Judy, and D. Markovic, "Comparison of spike-sorting algorithms for future hardware implementation," in *Engineering in Medicine and Biology Society, EMBS.*, 2008, pp. 5015–5020.
- [7] —, "Spike sorting," *IEEE Signal Processing Magazine*, vol. 29, no. 1, p. 124, 2012.
- [8] E. M. Glaser and W. B. Marks, "Separation of neuronal activity by waveform analysis," *Advances in Biomedical Engineering*, vol. 5, pp. 137–156, 1968.
- [9] J. C. Letelier and P. P. Weber, "Spike sorting based on discrete wavelet transform coefficients," *Journal of Neuroscience Methods*, vol. 101, no. 2, pp. 93–106, 2000.
- [10] M. S. Lewicki, "A review of methods for spike sorting: the detection and classification of neural action potentials," *Network: Computation in Neural Systems*, vol. 9, no. 4, pp. R53–R78, 1998.
- [11] S. Takahashi, Y. Anzai, and Y. Sakurai, "A new approach to spike sorting for multi-neuronal activities recorded with a tetrode—how ICA can be practical," *Neuroscience Research*, pp. 265–272, 2003.
- [12] C. Zhang, X. Zhang, M. Q. Zhang, and Y. Li, "Neighbor number, valley seeking and clustering," *Pattern Recognition Letters*, vol. 28, no. 2, pp. 173–180, 2007.
- [13] M. Blatt, S. Wiseman, and E. Domany, "Superparamagnetic clustering of data," *Phys. Rev. Lett.*, vol. 76, pp. 3251–3254, 1996.
- [14] D. Gabor, "Theory of communication. part I: The analysis of information," *Electrical Engineers-Part III: Radio and Communication Engineering, Journal of the Institution of*, pp. 429–441, 1946.
- [15] L. B. Jackson *et al.*, *Digital filters and signal processing*. Springer, 1989, vol. 3.
- [16] S. Mukhopadhyay and G. Ray, "A new interpretation of nonlinear energy operator and its efficiency in spike detection," *IEEE Transactions on Biomedical Engineering*, vol. 45, pp. 180–187, 1998.
- [17] H. W. Lilliefors, "On the kolmogorov-smirnov test for normality with mean and variance unknown," *Journal of the American Statistical Association*, vol. 62, no. 318, pp. 399–402, 1967.
- [18] R. Quiroga, Z. Nadasdy, and Y. Ben-Shaul, "Unsupervised spike detection and sorting with wavelets and superparamagnetic clustering," *Neural Comput.*, vol. 16, pp. 1661–1687, 2004.
- [19] M. Blatt, S. Wiseman, and E. Domany, "Data clustering using a model granular magnet," *Neural Comput.*, vol. 9, pp. 1805–1842, 1997.
- [20] *Fuglevand Laboratory of motor control neurophysiology*, Department of Physiology, University of Arizona, USA.
- [21] C. J. V. Rijsbergen, *Information Retrieval*, 2nd ed. Newton, MA, USA: Butterworth-Heinemann, 1979.